

## First Observation of Ion Acoustic Waves Produced by the Langmuir Decay Instability

S. Depierreux,<sup>1</sup> J. Fuchs,<sup>1</sup> C. Labaune,<sup>1</sup> A. Michard,<sup>1</sup> H. A. Baldis,<sup>2</sup> D. Pesme,<sup>3</sup> S. Hüller,<sup>3</sup> and G. Laval<sup>3</sup>

<sup>1</sup>Laboratoire pour l'Utilisation des Lasers Intenses, UMR 7605 CNRS-École Polytechnique-CEA-Université Paris VI, École Polytechnique, 91128 Palaiseau Cedex, France

<sup>2</sup>Institute for Laser Science and Applications (ILSA), Lawrence Livermore National Laboratory, P.O.B. 808, Livermore, California 94550

<sup>3</sup>Centre de Physique Théorique, UMR 7644 CNRS-École Polytechnique, École Polytechnique, 91128 Palaiseau Cedex, France

(Received 22 July 1999)

Thomson scattering measurements are presented which demonstrate conclusively the occurrence of the Langmuir decay instability (LDI) in a laser-produced plasma experiment. Both products of the instability, the ion acoustic wave and the electron plasma wave, were simultaneously observed and identified with their spectral characteristics. The secondary decay of the LDI-generated electron plasma wave, into another Langmuir wave and an ion acoustic wave, has been observed for the first time. The connection with growth and saturation of the stimulated Raman instability is discussed.

PACS numbers: 52.35.Fp, 52.35.Mw, 52.35.Ra, 52.40.Nk

Stimulated Raman scattering (SRS) is an important non-linear process in the context of inertial confinement fusion (ICF), because it can affect the coupling between the laser beams and the target [1]. In SRS, the incident electromagnetic (EM) wave decays into a scattered EM wave and an electron plasma wave (EPW) also called a Langmuir wave. The scattered light reduces the absorption efficiency, and the EPWs reduce the target gain by producing high energy electrons that preheat the core. According to linear theory of absolutely unstable SRS, the daughter waves should grow exponentially in time to very high levels with a growth rate depending on the incident intensity. However, the characteristic growth time is short compared to the laser pulse duration so that SRS behavior is dominated by saturation processes. Consequently, the control of SRS in ICF experiments requires the identification of the saturation processes and the prediction of the saturation levels.

Theoretical work and numerical simulations [2,3] predict that the parametric decay of the EPWs driven by SRS can play an important role in the SRS nonlinear saturation by introducing an additional damping on the EPWs. The three-wave Langmuir decay instability (LDI) is the decay of a primary Langmuir wave into a secondary more-or-less antiparallel Langmuir wave and a more-or-less parallel ion acoustic wave (IAW). Recent experiments have conjectured the occurrence of LDI to explain the dependence of the SRS reflectivity on the IAW damping rate [4,5]. EPWs traveling antiparallel to the laser wave vector have indeed been observed [6] and were attributed to LDI. However, these EPWs could also be explained in some other way, such as by the EPW reflection in local plasma density fluctuations. Therefore the best way to clear up any ambiguity and to demonstrate convincingly the occurrence of LDI is to observe simultaneously its two products, namely, the associated next-step secondary EPWs and IAWs with frequencies and wave numbers matching the resonance conditions with the instability. Here we report the observation

of IAWs resonantly produced by LDI, fully confirming the presence of LDI linked to SRS.

In this paper, we present the first observation of IAW produced by the LDI of the primary EPW generated by SRS. Thomson scattering from IAWs, with resolutions in wavelength and wave number, provides a complete set of information that allows the IAWs to be clearly identified as one of the LDI products and is therefore a more powerful LDI diagnostic than previously reported scattering from EPWs. The frequency and wave number spectra are found to be peaked at values corresponding very well to the combined resonance conditions for SRS and LDI. The peaked character of these spectra rules out all the other possible origins of these IAWs, such as the beating of oppositely directed EPWs produced in a filament plasma cavity or as the result of IAW turbulence. The high spectral resolution also provides the first evidence of cascade by separating the two counterpropagating IAWs, one (IAW2) produced (with EPW2) by the initial LDI decay of the SRS driven primary EPW (i.e., EPW1), and another by subsequent LDI decay of the secondary EPW (i.e., EPW2). The other new component of this experiment is the connection between measured SRS reflectivities and the direct observation of LDI (rather than the previous indirect connection between SRS and stimulated Brillouin scattering (SBS) or IAW damping conditions).

Five beams of the LULI (Laboratoire pour l'Utilisation des Lasers Intenses) facility were used to study the interaction between a 1.053  $\mu\text{m}$  wavelength ( $\omega_0$ ) laser beam, smoothed with a random phase plate (RPP), and a preformed underdense plasma. The plasma was formed by two counterpropagating laser beams incident on 380  $\mu\text{m}$  diameter CH (parlylene) disks of thickness 0.94  $\mu\text{m}$ , and heated by a third, identical beam, delayed by 0.5 ns with respect to the first two. The plasma formation beams were propagated through RPPs that produced a focal spot larger than the target. The targets were sufficiently thin as to

achieve a high-temperature plasma before the arrival of the interaction and probe laser beams. The interaction beam was focused along the principal axis of plasma expansion and delayed by 1.4 ns with respect to the plasma formation pulses. Using an  $f/3$  lens and an RPP consisting of a circular array of 2 mm elements, the focal spot diameter was  $160 \mu\text{m}$  FWHM (full width at half maximum), producing a peak average intensity of  $3.5 \times 10^{14} \text{ W/cm}^2$ . A layout of the beam configuration is shown in Fig. 1(a).

The Thomson scattering probe was synchronous with the interaction beam and was focused with a combination of a lens and an RPP with elongated elements, to form a focal region  $100 \mu\text{m}$  by  $1 \text{ mm}$  along the axis of the interaction beam. The Thomson scattered light was collected by a parabolic mirror and imaged onto two spectrometer–streak camera combinations by spherical mirrors. The geometry of the Thomson scattering diagnostic was chosen to preferentially collect the light from primary EPWs generated by backward SRS, and secondary EPWs and IAWs associated with backward LDI. Using the matching conditions for LDI:  $\omega_{\text{EPW1}} = \omega_{\text{EPW2}} + \omega_{\text{IAW2}}$  and  $\vec{k}_{\text{EPW1}} = \vec{k}_{\text{EPW2}} + \vec{k}_{\text{IAW2}}$ , where  $\omega_i$  and  $\vec{k}_i$  are the frequencies and wave numbers of the pump (EPW1), the secondary Langmuir waves (EPW2) and ion acoustic waves (IAW2), the wave numbers of the secondary EPW and IAW are  $|\vec{k}_{\text{EPW2}}| = |\vec{k}_{\text{EPW1}}| - \Delta k$  and  $|\vec{k}_{\text{IAW2}}| = 2|\vec{k}_{\text{EPW1}}| - \Delta k$ , respectively, with  $\Delta k = (2/3) \times k_D (Zm_e/m_i)^{1/2}$ , where  $k_D$  is the inverse Debye length [7]. Because  $\Delta k$  is only a few percent of  $k_{\text{EPW1}}$ , the Thomson down-shifted scattered light off EPW1 ( $\omega_{\text{down}} = \omega_{\text{probe}} - \omega_{\text{EPW1}}$ ,  $\vec{k}_{\text{down}} = \vec{k}_{\text{probe}} - \vec{k}_{\text{EPW1}}$ ) and the Thomson up-shifted scattered light off EPW2 ( $\omega_{\text{up}} = \omega_{\text{probe}} + \omega_{\text{EPW2}}$ ,  $\vec{k}_{\text{up}} = \vec{k}_{\text{probe}} + \vec{k}_{\text{EPW2}} \approx \vec{k}_{\text{down}}$ ) were emitted in very nearly the same direction and were recorded on the same diagnostic. Figure 1(b) shows diagrams of the wave vectors involved in SRS and LDI decays as well as in Thomson scattering. The spectral and temporal resolutions of the EPW system were  $30 \text{ \AA}$  and

50 ps, respectively. Scattered light off IAWs was recorded with a different system having a high spectral resolution,  $0.2 \text{ \AA}$ , and 60 ps of temporal resolution.

The plasma was characterized using time-resolved spectra of thermal Thomson scattering and Thomson scattered spectra of SRS driven EPWs. The electron temperature was  $0.7 \pm 0.1 \text{ keV}$  during the interaction pulse, and the electron density at the peak of the plasma profile evolved from  $0.45n_c$  to  $0.05n_c$  (where  $n_c = 1 \times 10^{21} \text{ cm}^{-3}$  is the critical electron density at  $\omega_0$ ). The scale length of the parabolic profile of the plasma was  $700 \mu\text{m}$ .

The first interesting result is the observation of scattered light off IAW having the wave vector of IAW2, being that predicted by the combined conservation laws of the SRS decay and the first LDI decay. Masks were used on both the probe beam and the collecting optics to select scattered light off IAW with well-defined wave vectors. A peak in the  $k$  spectrum was clearly observed for wave vector amplitudes between  $2.7\omega_0/c$  and  $3.1\omega_0/c$ . These waves correspond to the IAW (IAW2) produced by the decay in the backward direction of the primary EPW generated inside a  $40^\circ$  aperture cone round the backward SRS direction, at an electron density between  $0.1n_c$  and  $0.15n_c$ . The peak in the  $k$  spectrum rules out ion acoustic turbulence, which is another possible source of nonthermal IAW. An example of time-resolved spectra is shown in Fig. 2(a). The two pairs of signals observed are scattered light emitted at  $90$  and  $250 \mu\text{m}$  in the front part of the plasma and collected by the two slits of the streak camera [8]. The two signals in the right part of the frame are the expected IAW2 with frequencies down shifted from  $\omega_{\text{probe}}$  ( $3\omega_0$ ) by the IAW2 frequency ( $\omega_{\text{IAW2}} = k_{\text{IAW2}}c_s + \vec{k}_{\text{IAW2}} \cdot \vec{u}$ , where  $c_s$  is the sound speed, and  $\vec{u}$  is the flow velocity). The maximum of signal was produced in the front part, at  $\sim 150 \mu\text{m}$  from the summit of the profile, and occurred during the second half of the interaction pulse, coincident in time and location with the SRS activity. Typically, the density fluctuations ( $\delta n/n$ ) associated with the IAW2 are smaller than those associated with stimulated Brillouin scattering by a factor of 10 or so, and are in the range of  $10^{-3}$ .

The second and very significant result is the observation of an up-shifted component for each slit of the streak camera. These two signals can be seen in the left part of the frame of Fig. 2(a). They correspond to Thomson scattering from IAWs such as IAW3 propagating in the direction opposite to the IAW2 and having similar spectral characteristics. As expected, the frequency separation between the peaks of the signals ( $4.1 \text{ \AA}$ ) is twice the frequency of the sound wave calculated with the IAW2 wave number without flow effects (which cancel when the frequency of IAW2 and IAW3 are summed), with  $T_e = 0.7 \text{ keV}$ . Such IAWs correspond to theoretical predictions [9] and numerical simulations [2,3] which demonstrate that the EPW (EPW2) generated by the LDI of the EPW1 driven by SRS can subsequently be unstable with regards to a secondary

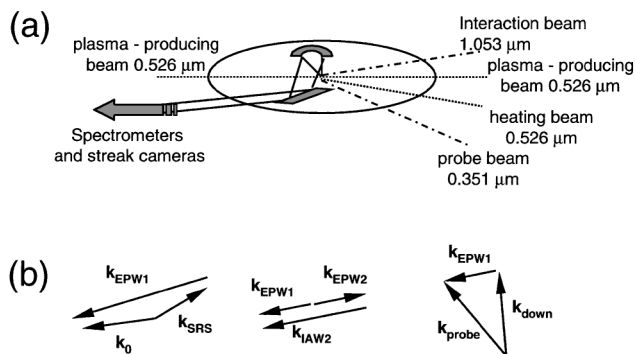


FIG. 1. (a) Layout of the beam configuration. All beams are in the horizontal plane with 600 ps FWHM (full width at half maximum) Gaussian pulses. (b) Wave-vector diagrams for the SRS of the interaction beam (left), the LDI of the electron plasma waves produced by SRS (center), and Thomson scattering of the probe beam (right).

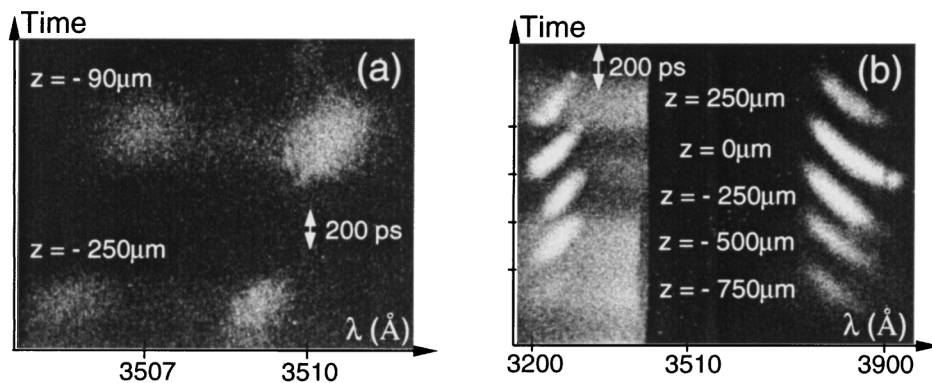


FIG. 2. (a) Time-resolved spectra of up and down Thomson scattered light off IAW2 and IAW3. IAW2 are ion acoustic waves produced by the Langmuir decay of electron plasma waves associated with stimulated Raman scattering (EPW1). IAW3 are ion acoustic waves produced by the Langmuir decay of the secondary electron plasma waves (EPW2). Direction  $z$  corresponds to the propagation of the interaction beam, with the minus sign referring to the front part of the plasma and  $z = 0$  being the summit of the profile. (b) Time-resolved spectra of up and down Thomson scattered light off EPW1 and EPW2. EPW1 are electron plasma waves produced by SRS. EPW2 are electron plasma waves produced by LDI of EPW1. Different optical attenuations have been used for the ten signals, allowing the observations of EPW1 and EPW2 at five different regions of plasma located along the laser axis, from  $z = -750 \mu\text{m}$  (in the front) to  $z = 250 \mu\text{m}$  (in the back).

LDI and decay into an EPW (EPW3) and an IAW (IAW3). This process may continue, producing Langmuir modes  $\text{EPW}(n+1)$  at  $|\vec{k}_{\text{EPW}}^{n+1}| = |\vec{k}_{\text{EPW}}^n| - \Delta k$ , propagating in opposite directions and ion acoustic waves  $\text{IAW}(n+1)$  at  $\vec{k}_{\text{IAW}}^{n+1} = \vec{k}_{\text{EPW}}^n - \vec{k}_{\text{EPW}}^{n+1}$ , thus generating the so-called LDI cascade. It may also give rise to Langmuir turbulence, depending on the electron temperature. In the regime of moderate electron temperature considered here, it can be expected on the basis of numerical simulations [3] carried out for homogeneous plasmas that the first steps of the LDI cascade may coexist with Langmuir turbulence. An excellent correlation was observed between the amplitudes of the IAW3 and the IAW2, with an amplitude ratio of 0.67 for laser intensities around  $(1-3) \times 10^{14} \text{ W/cm}^2$ . We consequently conclude that the two signals observed for each slit are produced by Thomson up and down scattering off the  $\text{IAW}(2p)$  and  $\text{IAW}(2p+1)$  produced by the first pair of steps ( $p=1$ ) of the LDI cascade.

Thomson scattered light off the primary and secondary EPWs was recorded during the same experiment. An example of time-resolved spectra showing light emitted by five different regions of plasma is shown in Fig. 2(b). For each location, we observed the down-shifted Thomson scattered light off primary EPW and the up-shifted Thomson scattered light off secondary EPW. We observed a strong dependence of the amplitude of the secondary EPW (EPW2) on the EPW1 amplitude [see Fig. 3(a)] and a good correlation between the amplitudes of EPW2 and IAW2 [see Fig. 3(b)] demonstrating that both EPW2 and IAW2 are produced by the Langmuir decay of the EPW1. It is the observation of IAW2 with the correct spectral signatures that rules out all other possible origins of EPW2, such as (i) optical mixing with background IAW fluctuations, (ii) partial reflection of EPW1 due to a local plasma density dip, or (iii) generation by an electron beam propagating backward to the laser light.

The second stage of our study was to investigate the influence of LDI upon the growth of SRS. The backscattered Raman light was collected in the focusing lens of the interaction beam and measured as a function of the laser intensity. The results are shown in Fig. 4(a). From the measured Thomson scattered light off EPW1, we deduced the density fluctuations associated with SRS as shown in Fig. 4(b). From the observation of EPW2 at low laser intensities, we may conclude that LDI takes place even for small levels of SRS, i.e., in the domain where we do not yet see clear signs of nonlinear saturation for the reflectivity as a function of the incident intensity.

In order to connect the occurrence of LDI with the SRS reflectivity behavior, we have developed the following scenario, consistent with numerical results [2,3] carried out for homogeneous plasmas. First of all, the laser intensities corresponding to our experimental results lie all in the regime of absolute instability for SRS in the spatial

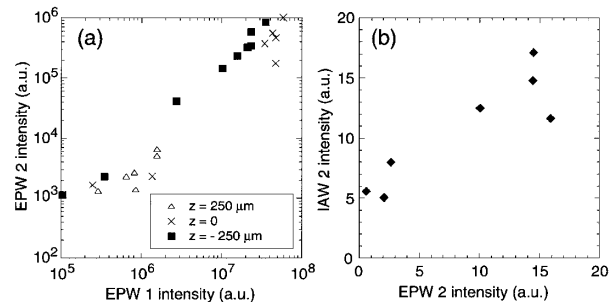


FIG. 3. (a) Thomson scattered intensity off EPW2 as a function of Thomson scattered intensity off EPW1. This had been done by varying the incident laser intensity from  $9.8 \times 10^{13}$  to  $3.4 \times 10^{14} \text{ W/cm}^2$  (b) Thomson scattered intensity off IAW2 as a function of Thomson scattered intensity off EPW2. This curve corresponds to incident laser intensities in the range  $(3-3.4) \times 10^{14} \text{ W/cm}^2$ .

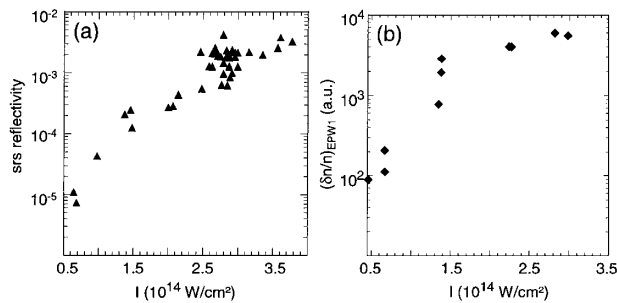


FIG. 4. (a) SRS backward reflectivity as a function of laser intensity. (b) Density fluctuations  $(\delta n/n)_{EPW1}$  associated with SRS as a function of laser intensity, for  $z = -250 \mu\text{m}$  in the front.

domain  $n_e/n_c > 0.07$ , since the conditions [10] for absolute instability related to the plasma inhomogeneity are satisfied. In the region of the density maximum, this condition reduces to  $I_{14} > 1.3$ , where  $I_{14}$  denotes the mean laser intensity  $I$  (i.e., its average value over the speckle distribution) in units of  $10^{14}$  W/cm<sup>2</sup>. In the other regions where the phase mismatch locally scales linearly with  $z$ , SRS would only be convectively unstable, with a linear gain too small to explain our experimental results. This would hold in the absence of local density profile modifications. The latter, however, occur because the laser field in the interaction volume, generated by an RPP, consists of speckles, the most intense of which have up to 12 times the average intensity  $I$  for our experimental parameters. For this reason, a significant number of speckles undergo self-focusing (SF) whenever  $I$  exceeds a threshold  $I_{SF}$ , which, for  $n_e/n_c = 0.08$ , reads  $I_{14} > I_{14SF} = 0.3$  in the above units. For the moderate electron temperatures considered here, the SF speckles experience an enhancement of their peak intensity [11] and induce a density depletion sufficiently large to give rise to local dips [12]. In these density dips, SRS develops via absolute instability [13], thus leading to a large local growth of the EPW1 amplitude. Within a short period, the LDI threshold is then greatly exceeded in these SF speckles, leading to the first steps of the LDI cascade (eventually together with Langmuir turbulence). This is why LDI occurs simultaneously as SRS, namely, in the regime  $I > I_{SF}$ . The SRS behavior is nonlinearly saturated in these SF speckles, so that the magnitudes of their individual reflectivities are in the order of a fraction of unity. The higher the mean laser intensity, the greater is the number of SF speckles. More precisely, nonlinear estimates similar to those made for SRS in self-focused speckles [14] lead to SRS reflectivities which are in the same order of magnitude as those observed in the range  $I_{14SF} < I_{14} \leq 1.5$ . Numerical simulations describing SRS in an inhomogeneous plasma irradiated by an RPP laser field are obviously needed to go further in with these estimates.

In summary, the occurrence of the Langmuir decay instability and of the first steps of the LDI cascade in laser-plasma interaction has been demonstrated by the simultaneous observation of the two LDI products and

their subsequent decays. The IAW spectra have been found to be peaked at values corresponding to the combined resonance conditions for SRS and LDI. These peaked spectra eliminate all the mechanisms of generation of observed EPW and IAW other than LDI. Theoretical estimates lead to a scenario along which SRS is taking place in the self-focused speckles only. In the latter, SRS is locally nonlinearly saturated by LDI and its subsequent cascade, but the fact that the number of self-focused speckles increases with laser intensity prevents one from observing the nonlinear saturation of the overall reflectivity.

The authors gratefully acknowledge the support of the technical groups of LULI and would like to thank H. Rose, W. Rozmus, and V. Tikhonchuk for enlightening discussions on nonlinear saturation of SRS. This work was partially supported under the auspices of the U.S. Department of Energy by the Lawrence Livermore National Laboratory under Contract No. W-7405-ENG-48. Part of this support was provided through the LLNL-LDRD program under the Institute for Laser Science and Applications.

- [1] W.L. Kruer, *The Physics of Laser Plasma Interactions* (Addison Wesley, Redwood City, CA, 1988); H. A. Baldis, E.M. Campbell, and W.L. Kruer, in *Physics of Laser Plasmas*, Handbook of Plasma Physics (North-Holland, Amsterdam, 1991), pp. 361–434; D. Pesme and C. Labaune, in *La Fusion Thermonucleaire Inertielle par Laser*, edited by R. Dautray and J.-P. Wateau (Eyrolles, Paris, 1993), Vol. 1.
- [2] S.J. Karttunen, *Phys. Rev. A* **23**, 2006 (1981); J. A. Heikkinen, and S. J. Karttunen, *Phys. Fluids* **29**, 1291 (1986); B. Bezzerides, D. F. DuBois, and H. A. Rose, *Phys. Rev. Lett.* **70**, 2569 (1993); T. Kolber, W. Rozmus, and V. T. Tikhonchuk, *Phys. Fluids B* **5**, 138 (1993); D. F. DuBois, H. A. Rose, and D. A. Russell, *Phys. Sci.* **T63**, 16 (1996); R. L. Berger *et al.*, *Phys. Plasmas* **5**, 4337 (1998).
- [3] D. A. Russell, D. F. DuBois, and H. A. Rose, *Phys. Plasmas* **6**, 1294 (1999).
- [4] R. P. Drake and S. H. Batha, *Phys. Fluids B* **3**, 2936 (1991); D. Villeneuve *et al.*, *Phys. Rev. Lett.* **71**, 368 (1993).
- [5] J. C. Fernández *et al.*, *Phys. Rev. Lett.* **77**, 2702 (1996); R. K. Kirkwood *et al.*, *Phys. Rev. Lett.* **77**, 2706 (1996); D. S. Montgomery *et al.*, *Phys. Plasmas* **5**, 1973 (1998).
- [6] C. Labaune *et al.*, *Phys. Plasmas* **5**, 234 (1998); K. L. Baker *et al.*, *Phys. Rev. Lett.* **77**, 67 (1996).
- [7] V. N. Oraevskii and R. Z. Sagdeev, *Sov. Phys. Tech. Phys.* **7**, 955 (1963).
- [8] H. A. Baldis and C. Labaune, *Rev. Sci. Instrum.* **67**, 451 (1996).
- [9] D. F. DuBois, H. A. Rose, and D. A. Russell, *Phys. Rev. Lett.* **66**, 1970 (1991).
- [10] M. N. Rosenbluth, *Phys. Rev. Lett.* **29**, 565 (1972).
- [11] S. Hüller, Ph. Mounaix, and V. T. Tikhonchuk, *Phys. Plasmas* **5**, 2706 (1998).
- [12] H. A. Rose and D. F. DuBois, *Phys. Fluids B* **5**, 590 (1993).
- [13] G. Picard and T. W. Johnston, *Phys. Fluids* **28**, 859 (1985).
- [14] V. T. Tikhonchuk, S. Hüller, and Ph. Mounaix, *Phys. Plasmas* **4**, 4369 (1997).